A Novel Signature Based on Pyroptosis-Related Genes for Predicting Breast Cancer

Shuang Shen
Zunyi Medical University https://orcid.org/0000-0002-0845-2533
Xin Chen
Zunyi Medical University
Rui Qu
Zunyi Medical University
Youming Guo
Zunyi Medical University
Yingying Su
Zunyi Medical University
Hang Jiang
Zunyi Medical University
Libo Luo (✉ llb13595381197@163.com)
Zunyi Medical University

Research

Keywords: pyroptosis, breast cancer, tumor immune microenvironment

Posted Date: May 24th, 2021

DOI: https://doi.org/10.21203/rs.3.rs-521609/v1

Abstract

Background: Breast cancer (BC) surpassed lung cancer as the most frequent malignant tumour in women. In recent years, pyroptosis has revealed itself as an inflammatory form of programmed cell death. However, it is unclear as to the expression of genes associated with pyroptosis in BC and its relationship to prognosis.

Results: In this study, we identified 31 pyroptosis regulators that are differentially expressed between BC and normal breast. The differently expressed genes (DEG) allow BC patients to be divided into three subtypes. Through single-factor and multi-factor COX regression and the application of least absolute contraction and selection operator (LASSO) Cox regression method, the survival prognostic value of each gene related to pyroptosis in The Cancer Genome Atlas (TCGA) cohort was evaluated, and a 4-gene signature was constructed. BC patients of the TCGA cohort are divided into low-risk or high-risk groups by risk score. The survival of the low-risk group was significantly higher than the high-risk group ($P < 0.001$). Using the median risk score from the TCGA cohort, BC patients from the Gene Expression Omnibus (GEO) cohort were divided into two risk sub-groups and similar conclusions were drawn. In combination with clinicopathological characteristics, the risk score is an independent predictive factor of OS in BC patients. Gene ontology (GO) and Kyoto Encylopedia of Genes and Genomes (KEGG) indicated that the high-risk group's immune genes were enriched and immune status was reduced.

Conclusions: In conclusion, pyroptosis-related genes are important for tumour immunity and can be used to predict the prognosis of BC.

Background

Breast cancer has become a key global public health concern and is the leading cause of cancer-related death in women.[1] In 2020, female breast cancer surpassed lung cancer as the most common type of cancer globally;[2] in the United States, breast cancer accounted for 30% of all female cancers in 2021, with 281,550 cases, while China accounts for 17.6% and 15.6% of the world's female breast cancer incidences and deaths, respectively.[3, 4, 5]

Breast cancer treatment is comprehensive, including surgery, endocrine therapy, radiotherapy and chemotherapy, targeted therapy, and immunotherapy. However, as the number of patients increases and tumors become increasingly drug-resistant, new treatment targets need to be identified to improve the clinical outcome of breast cancer. Therefore, there is an urgent need for reliable new models to predict and evaluate the effect of cancer treatment on patients.

Programmed cell death refers to death that relies on the regulation of genetic code within the cell.[6] There are two means of programmed cell death: apoptosis and pyroptosis. Apoptosis is a relatively thorough method of programmed death. Pyroptosis is an inflammatory programmed death method that is dependent on caspase 1, caspase 4, caspase 5, and caspase, and is mediated by the Gasdermin D (GSDMD) protein.[7] Infection and cell stress can trigger the assemblage of typical or atypical

inflammasomes, which activates caspase 1 and caspase 11. The activated caspase is cleaved by the GSDMD protein, transforming it into an activated state, resulting in cellular pyroptosis, which plays a key role in innate immunity.[8] Compared with other methods of cell death, the mechanism and morphological changes associated with cell death are different in pyroptosis. The most characteristic feature is that the process of cell death triggers an inflammatory response and is closely associated with many diseases. Generally, the occurrence and development of malignant tumors are determined by many factors, including the relative activity of proto-oncogenes and tumor suppressor genes, immune microenvironment, and inflammatory microenvironment. Given the pro-inflammatory nature of pyroptosis, it is related to the pathogenesis of many chronic inflammatory diseases.[9] Therefore, the inflammatory microenvironment formed by the release of a large number of inflammatory factors in the process of pyroptosis may promote the occurrence and development of tumors. Studies have found that NLRP3 and IL-18β, which it mediates, can promote the occurrence and development of inflammatory bowel disease (such as Crohn's disease and ulcerative colitis), and inflammatory bowel disease may eventually cause malignant tumors in the gastrointestinal tract.[10] Cell pyroptosis plays an important role in this process. Cell death may promote the occurrence and development of malignant tumors. Some studies have found that although the NF-κB signaling pathway is closely related to the occurrence and development of malignant tumors, the abnormal activation of the NF-κB signaling pathway allows cells to resist programmed cell death while simultaneously carrying out proliferation, invasion, and metastasis, thereby promoting malignancy, which leads to the occurrence and development of tumors.[11] However, inhibiting the activity of the NF-κB pathway can promote programmed cell death via pyroptosis and inhibit the occurrence and development of malignant tumors.[12]

As per current understanding, pyroptosis is closely related to the occurrence and development of a variety of malignant tumors. However, there are very few studies on the specific mechanism of cell pyroptosis in the treatment of breast cancer. Therefore, we have systematically studied the differences in expression of genes related to pyroptosis between the normal breast tissue and breast cancer tissue, explored the prognostic value of these genes, and studied the correlation between tumor immune microenvironment and pyroptosis.

Results

DEGs identification between normal tissue and tumor tissue

By comparing the expression levels of 113 normal tissues and 1103 breast cancer tissues from TCGA data with 33 pyroptosis-related genes, 19 differentially expressed genes ($P < 0.05$) were identified. Among them, nine genes are down-regulated and the other ten genes are up-regulated. The heatmap in Fig. 1A shows the RNA expression levels of these genes. Through protein–protein interaction network (PPI) analysis, the interaction of these pyroptosis-related genes is further explored and the results are presented in Fig. 1B. We found that CASP1, PYCARD, NLRP3, NLRC4, CASP5, NLRP1, AIM2, IL1B, and IL18 are hub genes (Fig. 1C). Except for NLRC4 and CASP5, others are DEGs between normal tissue and breast tumor tissue. Figure 1D shows the network of all genes related to pyroptosis.

Tumor classification based on DEGs

To explore the relationship between the expression of 19 pyroptosis-related DEGs and breast cancer subtypes, we performed a consensus cluster analysis on 1085 breast cancer patients with complete follow-up information in the TCGA cohort. By increasing the clustering variable (k) from 2 to 9, we found that when k = 3, the intra-group correlation is highest and the inter-group correlation is low. This indicates that the 1085 breast cancer patients can be divided into three clusters based on 31 DEGs (Figure 2A). Gene expression profile and clinical characteristics, including Age, Stage, ER (estrogen receptor) status, PR (progesterone receptor) status, HER2 (human epidermal growth factor receptor 2) status, Subtype, age (≤60 years or> 60 years old), and Subtype are shown in the heat map, but there is a difference between the three clusters. There is almost no difference in clinical characteristics (Figure 2B). The overall survival time between the three clusters was also compared, but no significant difference was found (P = 0.09, Figure 2C).

Establishment of prognostic gene model based on TCGA cohort

A total of 1035 breast cancer samples were matched to the corresponding patients with complete survival information. Univariate Cox regression analysis was used for the preliminary screening of survival-related genes. The eight genes (CASP1, CASP4, CASP8, CASP9, ELANE, GPX4, IL18, and PYCARD) that meet the criteria P <0.2 are retained for further analysis. These eight genes have HRs <1 and are all protective genes (Figure 3A)). By performing Least Absolute Shrinkage and Selection Operator (LASSO) Cox regression analysis, the markers of four genes were constructed according to the optimal λ value (Figure 3B, C). The risk score was calculated as follows: risk score = (−0.173×CASP9 exp.) + (−0.122×ELANE exp.) +(−1.239×GPX4 exp.) +(−0.052×IL18 exp.). Based on the median risk score, 1034 patients were divided into low-risk and high-risk groups (Figure 3D). Principal component analysis (PCA) showed that patients with different risks were satisfactorily divided into two clusters (Figure 3E). Patients in the high-risk group had more deaths and shorter survival times than those in the low-risk group (Figure 3F). Analysis of the Kaplan-Meier survival curve showed that the OS time between the two groups was significantly different (P <0.001, Figure 3G). Through a time-dependent receiver operating characteristics (ROC) analysis to evaluate the sensitivity and specificity of the prognostic model, we found that the area under the ROC curve (AUC) was 0.620 in three years, 0.619 in five years, and 0.644 in seven years (Figure 3H).

External verification of the risk model

We selected 390 breast cancer patients from the GEO cohorts (GSE7390, N=198; GSE42568, N=104; GSE20713, N=88) as the validation set. Before further verification, gene expression data were normalized and batch effects were removed. According to the median risk score of the TCGA cohort, patients in the three GEO cohorts were divided into high- and low-risk groups. (GSE7390: 113 cases of low risk, 85 cases of high risk; GSE42568: 22 cases of low risk, 82 cases of high risk; GSE20713: 23 cases of low risk, 65 cases of high-risk, as shown in Figure 4A, B, C). The PCA of three datasets (GSE7390, GSE42568, and GSE20713) shows satisfactory separation between the two subgroups, as illustrated in Figure 4D, E, F. In

addition, we found that low-risk patients have longer survival times and lower mortality than high-risk patients as illustrated in Figure 4G, H, I. The Kaplan–Meier analysis of the three GEO cohorts indicates that there were significant differences in OS between the low-risk and high-risk groups (all $p < 0.01$, Figure 4J, K, L). The ROC curve analysis of three GEO cohorts shows that our model has good predictive performance (Figure 4M, N, O).

Independent prognostic analysis of risk models

To evaluate whether the risk assessment of our model can be used as an independent prognostic factor, we used univariate and multivariate COX regression analysis methods. Univariate Cox regression analysis showed that in the TCGA, GSE7390, and GSE42568 cohorts, a risk score can be used as an independent factor for low survival (HR = 4.359, 95% CI: 1.694–11.221, HR: 9.129, 95% CI: 2.379–35.029 and HR: 12.190, 95% CI: 1.938–76.667 (Figure 5A, C, E). Concurrently, in the above three cohorts, multivariate COX analysis showed that our risk score was an independent prognostic factor (HR = 3.804 95% CI: 1.520–9.518, HR: 7.725, 95% CI: 2.045–29.183 and HR: 14.685, 95% CI: 2.502–86.180, Figure 5B, D, F). In the other cohort (GSE20713), we found that risk score cannot be used as a prognostic factor. We also drew a clinical heatmap of the TCGA cohort using the R package *ComplexHeatmap*. We found that the two clinical indicators of T stage and HER2 status were different between the high- and low-risk groups ($p<0.05$). (Figure 5G)

GO and KEGG analysis based on the risk model

To further explore the differences in gene function and pathways between groups, we extracted DEGs through the R package limma and set the threshold as FDR <0.05 and $|\log2FC| \geq 1$. We identified 278 DEGs between the high- and low-risk groups in the TCGA cohort, of which 267 genes were down-regulated and 11 genes were up-regulated (data are listed in Table S3). GO enrichment analysis and KEGG pathway analysis were performed on these DEGs. The results indicate that DEGs are mainly related to immune response, immune response-activating cell surface receptor signaling pathway, and Cytokine–cytokine receptor interaction (Figure 6A, B).

Comparison of immunological activity between subgroups

Through functional analysis, we further compared the enrichment scores of 16 types of immune cells and the activity enrichment analysis of 13 immune-related pathways (ssGSEA) between the TCGA cohort and the high- and low-risk patients in the three GEO cohorts by using a single-sample genome. In the TCGA cohort, we found that among the 16 immune cell types, the low-risk group had a higher number of immune cells, especially ADCs, B cells, CD8+ T_cells, DCs, IDCs, Mast_cells, Neutrophils, NK_cells, pDCs, T_helper_cells, Tfh, Th1_cells, Th2_cells, and TILTreg. (Figure 7A, B) Compared with the high-risk group, the low-risk group demonstrated higher activity in 13 immune pathways. When evaluating the immunization status of the three GEO cohorts, similar conclusions were reached. (Figure 7C, D, E, F, G, H)

Correlation analysis between chemotherapeutic drugs and model

We sought to determine the association between risk and the efficacy of chemotherapy in breast cancer treatment in the TCGA cohort. We found that the low-risk group was associated with the lower half inhibitory concentration (IC50) of chemotherapy treatments, such as Paclitaxel, Doxorubicin, Gemcitabine, Cisplatin, and PD.0332991 (Palbociclib) , and the higher IC50 with Lapatinib. Thus, this model can be used as a predictive indicator of chemical drug sensitivity (Figure 8).

Discussion

In this study, we first analyzed the expression of 33 known pyroptosis-related genes at the mRNA level. We found that most of these genes are differentially expressed in breast cancer and normal adjacent tissues. To further explore the characteristics of these DEGs, we observed that there was no significant difference in the survival time and other clinical case characteristics in the three clusters generated by the consensus cluster analysis. To evaluate the prognostic value of these regulatory factors in breast cancer, we further screened out four genes related to pyroptosis through COX univariate analysis and LASSO COX regression. We also constructed a risk model, verified its efficacy through an external dataset, and obtained good results. Furthermore, we conducted a differential analysis of gene expression in the two subgroups of high and low risk. Functional analysis showed that these DEGs are related to immune response and immune-related pathways. We further compared the immune cell infiltration and activation pathways between the high- and low-risk subgroups. We found that compared with the high-risk group, the low-risk group had a higher level of infiltrating immune cells and demonstrated higher activity in immune-related pathways. We also tested the sensitivity of traditional chemotherapy drugs in the two subgroups. We found that compared with the low-risk group, patients in the high-risk group were less sensitive to these drugs. This finding could guide some clinical treatment decisions.

In recent years, owing to in-depth studies of the new programmed death procedure, pyroptosis has been discovered, which plays a dual role in the occurrence, development, and treatment of tumors.[13] On the one hand, the pro-inflammatory nature of pyroptosis is related to the pathogenesis of many chronic inflammatory diseases. Therefore, the inflammatory microenvironment formed by the release of a large number of inflammatory factors in the process of pyroptosis may promote the occurrence and development of tumors.[14] On the other hand, pyroptosis itself can stimulate or inhibit a variety of cell pathways, including programmed cell death featuring pyroptosis, and inhibit the occurrence and development of malignant tumors. In breast cancer research, there are few reports on the interactions between genes related to pyroptosis and their influence on the survival time and treatment effect of breast cancer patients. Our study found that the risk model constructed using four genes related to pyroptosis (IL18, ELANE, GPX4, and CASP9) can predict the OS of breast cancer patients. Interleukin 18 (IL18), originally called interferon-inducing factor (IFN-γ inducing factor or IGIF), belongs to the IL-1 family; it is structurally homologous to IL-1 but functionally similar to IL-12. It can induce IFN-γ production, activate natural killer (NK) cells and toxic T lymphocytes (CTL), and induce helper T cells (Th), thus playing an important role in the body’s anti-infection, anti-inflammatory, and anti-tumor processes. In the classic pathway of pyroptosis-related death,[15] the body is stimulated by various factors to activate the inflammasome. The activation of the inflammasome is one of the most important pathways in the

process of cellular natural immunity.[16] The activated inflammasome further activates caspase-1, which in turn promotes the maturation of the precursors of interleukin (IL)-1β and IL-18, recruits inflammatory cells, expands the inflammatory response, and leads to pyroptosis. Inflammation is considered a risk factor for cancer progression.[17] IL-18 is a pro-inflammatory cytokine that plays an important role in many inflammatory diseases and immune responses. It has an inseparable relationship with tumors, showing varying degrees of expression.[18] We found that it is highly expressed in tumor tissues, and it seems to be an oncogene. However, in our survival analysis, it was found that it is related to the survival of breast cancer patients because it is highly expressed in patients in our low-risk group. This contradictory finding is worthy of further research. Neutrophil-expressed elastase (ELANE) is one of the main serine proteases secreted by neutrophils,it can activate pro-inflammatory cytokines and play a key role in the immune response.[19] In the RNA study of 197 clear cell renal cell carcinomas (ccRCCs), Wei et al.[20] found that the ELANE gene may be related to the invasion and metastasis of ccRCCs and may be used as a prognostic and therapeutic biomarker for ccRCCs. In our study, we found that ELANE is differentially expressed in breast cancer tissues and normal adjacent tissues, and it is overexpressed in normal tissues. Therefore, we speculate that it may participate in the immune response process during tumorigenesis and inhibit the further development of tumors. However, its specific tumor-inhibiting mechanism needs to be further studied. Glutathione peroxidase 4 (GPX4) is a protein that mainly inhibits lipid peroxidation. In addition to its unique ability to reduce H2O2 and small molecular hydrogen peroxide, GPX4 can also reduce hydrogen peroxide in complex forms such as phospholipids and cholesterol.[21] GPX4 has been reported to be associated with many types of cancer. In gliomas, it is significantly overexpressed in tumor tissues and cell lines. It is found that GPX4 is involved in the migration, proliferation, and pyroptosis of glioma cells, while high expression of GPX4 has less impact on glioma patients.[22] In our study, no difference in GPX4 expression was found between tumor and normal tissues, or between high- and low-risk subgroups. Therefore, its specific mechanism for improving the OS of breast cancer patients needs to be further explored. Caspase 9 (CASP9) is a member of the family of coding cysteine-aspartic proteases (caspase). It can be proteolytically processed and activated by the protein complex of apoptotic bodies, cytochrome c, and apoptotic peptidase activating factor 1.[23] This is considered one of the earliest steps in the caspase activation cascade. This protein is believed to play a central role in pyroptosis and is a tumor suppressor. M Sharif et al.[24] found that in breast cancer, miR-182-5p can be inhibited by regulating the expression of CASP9, which can affect the proliferation and pyroptosis of tumor cells. Although we found no difference in the expression of CASP9 between tumors and normal tissues, it is positively correlated with the survival time of breast cancer patients, so it plays a role in suppressing cancer. In summary, in our risk model, four genes (IL18, ELANE, GPX4, and CASP9) that may be triggers for promoting pyroptosis are associated with better breast cancer OS. However, the interaction of these genes with pyroptosis and their potential to inhibit tumor development needs to be further studied.

Although pyroptosis is a major research hotspot, and some similarities with pyroptosis and some overlapping mechanisms have been found, the research on pyroptosis is still insufficient. As the tumor progresses, there may be multiple simultaneous cell death modes in the body that affect each other.[25]

For example, in our model, CASP9 plays a central role in pyroptosis. In this study, we analyzed DEGs between high- and low-risk groups through GO and KEGG and found that these DEGs are mainly involved in immune response and immune cell chemotaxis. Therefore, we speculate that the tumor immune microenvironment is regulated by these thermal apoptotic factors. Furthermore, it was found that the high-risk group in the TCGA cohort had a lower level of tumor-infiltrating immune cells, indicating that its immune function was generally impaired. This conclusion was further confirmed in the three GEO cohorts. Ye et al. also found similar results in ovarian cancer.[26] Based on these findings, we believe that the poor survival rate of high-risk breast cancer patients may be due to the body's reduced anti-tumor immunity.

At present, there are few studies on the mechanism of pyroptosis in breast cancer. Our study identified four genes with the ability to regulate pyroptosis, and further studied the prognostic value of these pyroptosis-related genes in breast cancer and provided theoretical support for future research. However, owing to a lack of data, we are unable to determine the role of these genes in the pathway of pyroptosis death in breast cancer. We will conduct in-depth research in this area in the future.

Conclusion

In conclusion, our research indicates that pyroptosis is closely related to breast cancer because in breast cancer tissues and normal tissues, most genes related to pyroptosis are differentially expressed. Furthermore, our risk model based on four genes related to pyroptosis can predict the survival status in the TCGA and GEO cohorts. The DEGs between the high- and low-risk groups are related to tumor immunity. Our research provides new genetic characteristics for predicting the prognosis of breast cancer patients and provides an important basis for future research on the relationship between pyroptosis-related genes and breast cancer immunity.

Methods

Dataset acquisition

Complete RNA sequences and clinical characteristics of patients from 113 normal cases and 1103 breast cancer cases were obtained from the TCGA BRCA project (https://tcga-data.nci.nih.gov/tcga/) on April 15, 2021. The external validation set data (GSE7390, GSE42568, and GSE20713) including RNA-seq data and clinical information files can be downloaded from the GEO website (https://www.ncbi.nlm.nih.gov/geo/). All patients were followed up for at least 30 days.

Identification of differentially expressed genes related to pyroptosis

We extracted 33 genes related to pyroptosis from previous studies.[27,28,29,30] These are listed in Table S1. We used the R package "limma" to identify differentially expressed genes (DEGs) with P values <0.05. Details of the DEGs are listed in Table S2. A PPI network for DEG was established through the online network tool STRING (https://string-db.org/).

Model construction and verification of pyroptosis-related genes

First, we used COX regression analysis to assess the correlation of pyroptosis-related genes to survival status in the TCGA dataset. During this step, we define the P value to 0.2 to avoid omissions. Eight genes linked to survival have been identified. We then applied lasso regression to refine the range of candidate genes and develop a prognostic model. As a result of this screening, four genes and their coefficients were identified. The penalty parameter (λ) was established based on the lowest standard. By concentrating and normalizing TCGA expression data and using formulas, the risk score was calculated. According to the median risk, TCGA patients were divided into low-risk and high-risk groups. The Kaplan-Meier survival curve was used for calculating and comparing survival differences between the two groups. ROC curve analysis was performed using the R package. PCA based on the 4-gene signature was performed through the "prcomp" function in the "stats" R package. The "survival", "survivor" and "time ROC" R software packages were used to perform a 3-year ROC curve analysis. For the validation study, the breast cancer cohort from the GEO database (GSE7390, GSE42568, and GSE20713) was used. The expression of each gene related to pyroptosis was also normalized by the "scale" function. Then the risk score was calculated by the same formula as the TCGA cohort. By applying the median risk score of the TCGA cohort, patients in the GSE cohort were also divided into low-risk or high-risk groups, and then these groups were compared to validate the risk model.

Independent prognostic analysis of risk score

We obtained the clinical information (age, TNM stage, Stage, ER, PR, HER2 status, and subtype) of patients in the TCGA cohort and information (age, ER, PR, HER2 status, and subtype data) of patients in the GEO cohorts, combined with the risk model, using which we established scoring. Univariate and multivariate COX regression analyses were performed.

Functional enrichment analysis of DEGs between low-risk and high-risk populations

Based on the median risk score, breast cancer patients in the TCGA cohort were divided into low-risk and high-risk groups. DEGs between the low-risk and high-risk groups was filtered. The filter criteria are $|\log2FC| \geq 0.5$ and FDR <0.05. GO and KEGG analysis was performed on DEG through the R package "cluster profile". The R package "gsva" was used to perform ssGSEA to calculate the fraction of infiltrating immune cells and evaluate the status of immune-related pathways.

Exploration of the significance of this model in clinical treatment

To evaluate this model in the clinical treatment of breast cancer, we used the R package "pRRophetic" to calculate the IC50 of commonly used chemotherapy drugs in the TCGA cohort. The NCCN guidelines suggest that anti-tumor drugs, such as Paclitaxel, Doxorubicin, Gemcitabine, Cisplatin, Lapatinib, and PD.0332991 (Palbociclib) be used for the treatment of breast cancer.

Statistical analysis

All processes are shown in Figure 9. One-way analysis of variance was used to compare gene expression levels between normal patients and breast cancer patients, and the Pearson chi-square test was selected as the categorical variable. The Kaplan–Meier method and two-way log-rank test were used to compare the OS of patients between subgroups. Univariate and multiple Cox regression models were used to evaluate the independent prognostic value of the risk model. Mann–Whitney test was used to compare the immune cell infiltration and immune pathway activation status between the two groups. Wilcoxon signed-rank test is used to compare IC50 differences between high- and low-risk groups.

Abbreviation

BC:breast cancer;DEG: differently expressed genes;TCGA:The Cancer Genome Atlas; GEO: Gene Expression Omnibus;GO:Gene ontology;KEGG:Kyoto Encylopedia of Genes and Genomes;GSDMD: the Gasdermin D protein;PPI:protein–protein interaction network; IC50:half inhibitory concentration;ER:estrogen receptor;PR:progesterone receptor;Her2:human epidermal growth factor receptor 2; LASSO:Least Absolute Shrinkage and Selection Operator;PCA:Principal component analysis; ROC:receiver operating characteristics ;AUC:area under curve. IL18:Interleukin 18;NK :natural killer cells; CTL:toxic T lymphocytes;ELANE:Neutrophil-expressed elastase;ccRCCs:clear cell renal cell carcinomas; GPX4:Glutathione peroxidase 4; CASP9:Caspase 9 .

Declarations

Ethics approval and consent to participate

TCGA and GEO belong to public databases. The patients involved in the database have obtained ethical approval. Users can download relevant data for free for research and publish relevant articles. Our study is based on open source data, so there are no ethical issues and other conflicts of interest.

Consent for publication

Not applicable.

Competing interests

The authors declare that they have no conflict of interest.

Funding

This research did not receive any specific grant from any funding agency in the public, commercial, or not-for-profit sector. Data Availability Statement

Author Contributions

Author contributions SS and XC conducted the formal analysis and wrote the original draft; SS, XC and LBL performed the project administration;HJ participated in software; YMG and YYS conducted data curation; RQ contributed to writing, reviewing, and editing the article. All authors approved the final manuscript as submitted and agree to be accountable for all aspects of the work.

Acknowledgments

We acknowledge TCGA and GEO database for providing their platforms and contributors for uploading their meaningful datasets.

Availability of data and material

Available upon request

References

1. Akram M, Iqbal M, Daniyal M, Khan AU. Awareness and current knowledge of breast cancer. Biol Res. 2017;50:33.
2. Sung H, Ferlay J, Siegel RL, Laversanne M, Soerjomataram I, Jemal A, et al., Global cancer statistics 2020: GLOBOCAN estimates of incidence and mortality worldwide for 36 cancers in 185 countries. CA Cancer J Clin (2021).
3. Siegel RL, Miller KD, Fuchs HE, Jemal A. Cancer Statistics 2021 CA Cancer J Clin. 2021;71:7–33.
4. Vardell E. Global Health Observatory Data Repository. Med Ref Serv Q. 2020;39:67–74.
5. Chen W, Zheng R, Baade PD, Zhang S, Zeng H, Bray F, et al. Cancer statistics in China, 2015. CA Cancer J Clin. 2016;66:115–32.
6. Galluzzi L, Vitale I, Aaronson SA, Abrams JM, Adam D, Agostinis P, et al. Molecular mechanisms of cell death: recommendations of the Nomenclature Committee on Cell Death 2018. Cell Death Differ. 2018;25:486–541.
7. Shi J, Gao W, Shao F. Pyroptosis: Gasdermin-Mediated Programmed Necrotic Cell Death. Trends Biochem Sci. 2017;42:245–54.

8. Xia S, Hollingsworth LT, Wu H. Mechanism and Regulation of Gasdermin-Mediated Cell Death. Cold Spring Harb Perspect Biol 12 (2020).
9. Liu Z, Gan L, Xu Y, Luo D, Ren Q, Wu S, et al., Melatonin alleviates inflammasome-induced pyroptosis through inhibiting NF-kappaB/GSDMD signal in mice adipose tissue. J Pineal Res 63 (2017).
10. Zaki MH, Lamkanfi M, Kanneganti TD. The Nlrp3 inflammasome: contributions to intestinal homeostasis. Trends Immunol. 2011;32:171–9.
11. Chen L, Li Q, Zheng Z, Xie J, Lin X, Jiang C, et al. Design and optimize N-substituted EF24 as effective and low toxicity NF-kappaB inhibitor for lung cancer therapy via apoptosis-to-pyroptosis switch. Chem Biol Drug Des. 2019;94:1368–77.
12. Kasparkova J, Thibault T, Kostrhunova H, Stepankova J, Vojtiskova M, Muchova T, et al. Different affinity of nuclear factor-kappa B proteins to DNA modified by antitumor cisplatin and its clinically ineffective trans isomer. Febs J. 2014;281:1393–408.
13. Gong W, Shi Y, Ren J. Research progresses of molecular mechanism of pyroptosis and its related diseases. Immunobiology. 2020;225:151884.
14. Xia X, Wang X, Zheng Y, Jiang J, Hu J. What role does pyroptosis play in microbial infection? J Cell Physiol. 2019;234:7885–92.
15. Nakanishi K. Unique Action of Interleukin-18 on T Cells and Other Immune Cells. Front Immunol. 2018;9:763.
16. Lin J, Cheng A, Cheng K, Deng Q, Zhang S, Lan Z, et al., New Insights into the Mechanisms of Pyroptosis and Implications for Diabetic Kidney Disease. Int J Mol Sci 21 (2020).
17. He X, Qian Y, Li Z, Fan EK, Li Y, Wu L, et al. TLR4-Upregulated IL-1beta and IL-1RI Promote Alveolar Macrophage Pyroptosis and Lung Inflammation through an Autocrine Mechanism. Sci Rep. 2016;6:31663.
18. Esmailbeig M, Ghaderi A. Interleukin-18: a regulator of cancer and autoimmune diseases. Eur Cytokine Netw. 2017;28:127–40.
19. Taylor S, Dirir O, Zamanian RT, Rabinovitch M, Thompson A. The Role of Neutrophils and Neutrophil Elastase in Pulmonary Arterial Hypertension. Front Med (Lausanne). 2018;5:217.
20. Wei Z, Wu B, Wang L, Zhang J. A large-scale transcriptome analysis identified ELANE and PRTN3 as novel methylation prognostic signatures for clear cell renal cell carcinoma. J Cell Physiol. 2020;235:2582–9.
21. Cozza G, Rossetto M, Bosello-Travain V, Maiorino M, Roveri A, Toppo S, et al. Glutathione peroxidase 4-catalyzed reduction of lipid hydroperoxides in membranes: The polar head of membrane phospholipids binds the enzyme and addresses the fatty acid hydroperoxide group toward the redox center. Free Radic Biol Med. 2017;112:1–11.
22. Zhao H, Ji B, Chen J, Huang Q, Lu X. Gpx 4 is involved in the proliferation, migration and apoptosis of glioma cells. Pathol Res Pract. 2017;213:626–33.

23. An HK, Chung KM, Park H, Hong J, Gim JE, Choi H, et al. CASP9 (caspase 9) is essential for autophagosome maturation through regulation of mitochondrial homeostasis. Autophagy. 2020;16:1598–617.
24. Sharifi M, Moridnia A. Apoptosis-inducing and antiproliferative effect by inhibition of miR-182-5p through the regulation of CASP9 expression in human breast cancer. Cancer Gene Ther. 2017;24:75–82.
25. Fritsch M, Gunther SD, Schwarzer R, Albert MC, Schorn F, Werthenbach JP, et al. Caspase-8 is the molecular switch for apoptosis, necroptosis and pyroptosis. Nature. 2019;575:683–7.
26. Ye Y, Dai Q, Qi H. A novel defined pyroptosis-related gene signature for predicting the prognosis of ovarian cancer. Cell Death Discovery. 2021;7:71.
27. Karki R, Kanneganti TD. Diverging inflammasome signals in tumorigenesis and potential targeting. Nat Rev Cancer. 2019;19:197–214.
28. Xia X, Wang X, Cheng Z, Qin W, Lei L, Jiang J, et al. The role of pyroptosis in cancer: pro-cancer or pro-"host"? Cell Death Dis. 2019;10:650.
29. Wang B, Yin Q. AIM2 inflammasome activation and regulation: A structural perspective. J Struct Biol. 2017;200:279–82.
30. Christgen S, Place DE, Kanneganti TD. Toward targeting inflammasomes: insights into their regulation and activation. Cell Res. 2020;30:315–27.

Supplementary

Table S2 is not available with this version

Figures

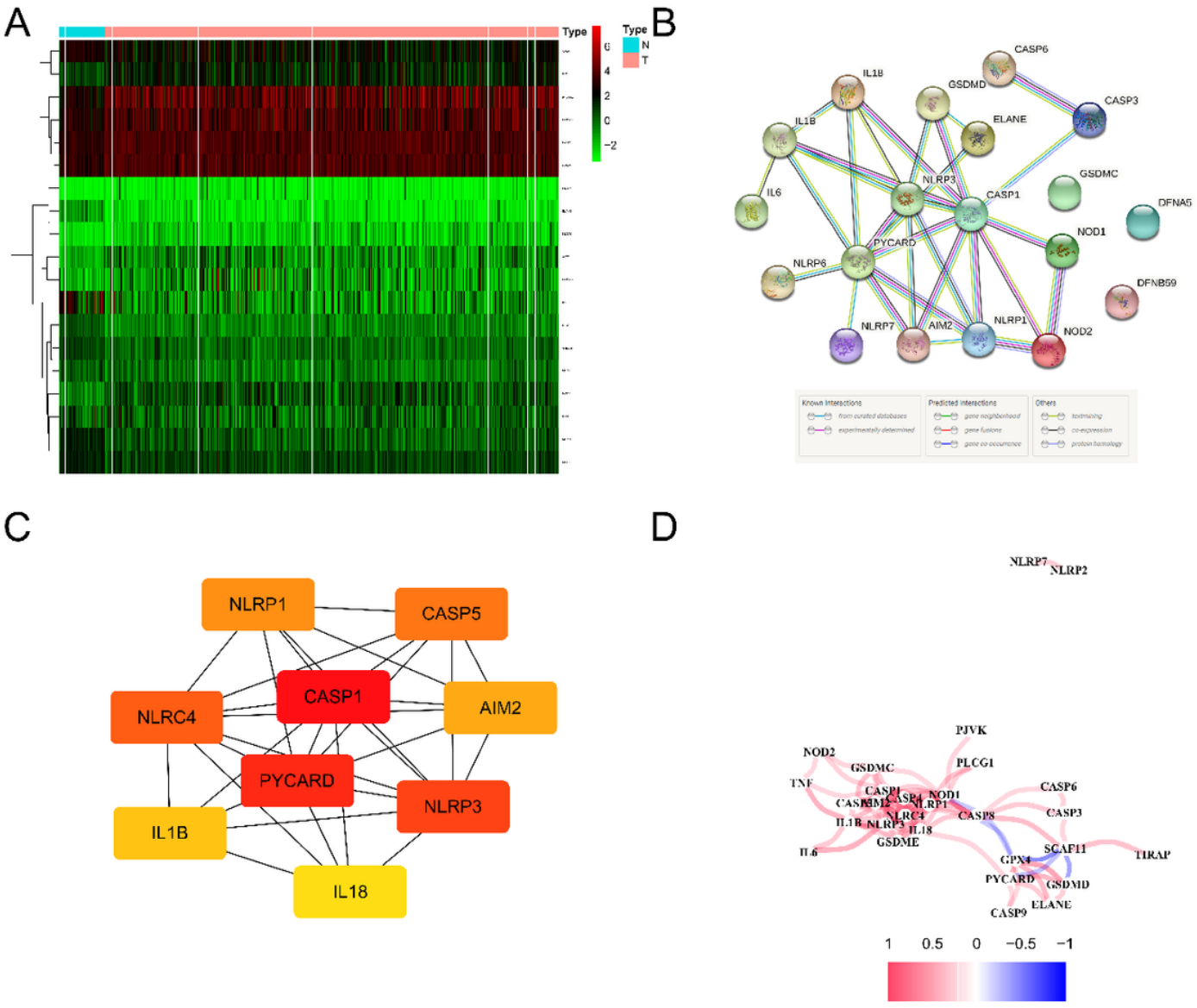

Figure 1

Expressions of the 33□19 DEGs□pyroptosis-related genes and the interactions among them. A Heatmap (green: low expression level; red: high expression level) of the pyroptosis-related genes between the normal (N, brilliant blue) and the tumour tissues (T, red). B PPI network showing the interactions of the pyroptosis-related genes (interaction score = 0.9).C The 9 Hub genes. D The correlation network of the pyroptosis-related genes (red line: positive correlation; blue line: negative correlation. The depth of the colours reflects the strength of the relevance)

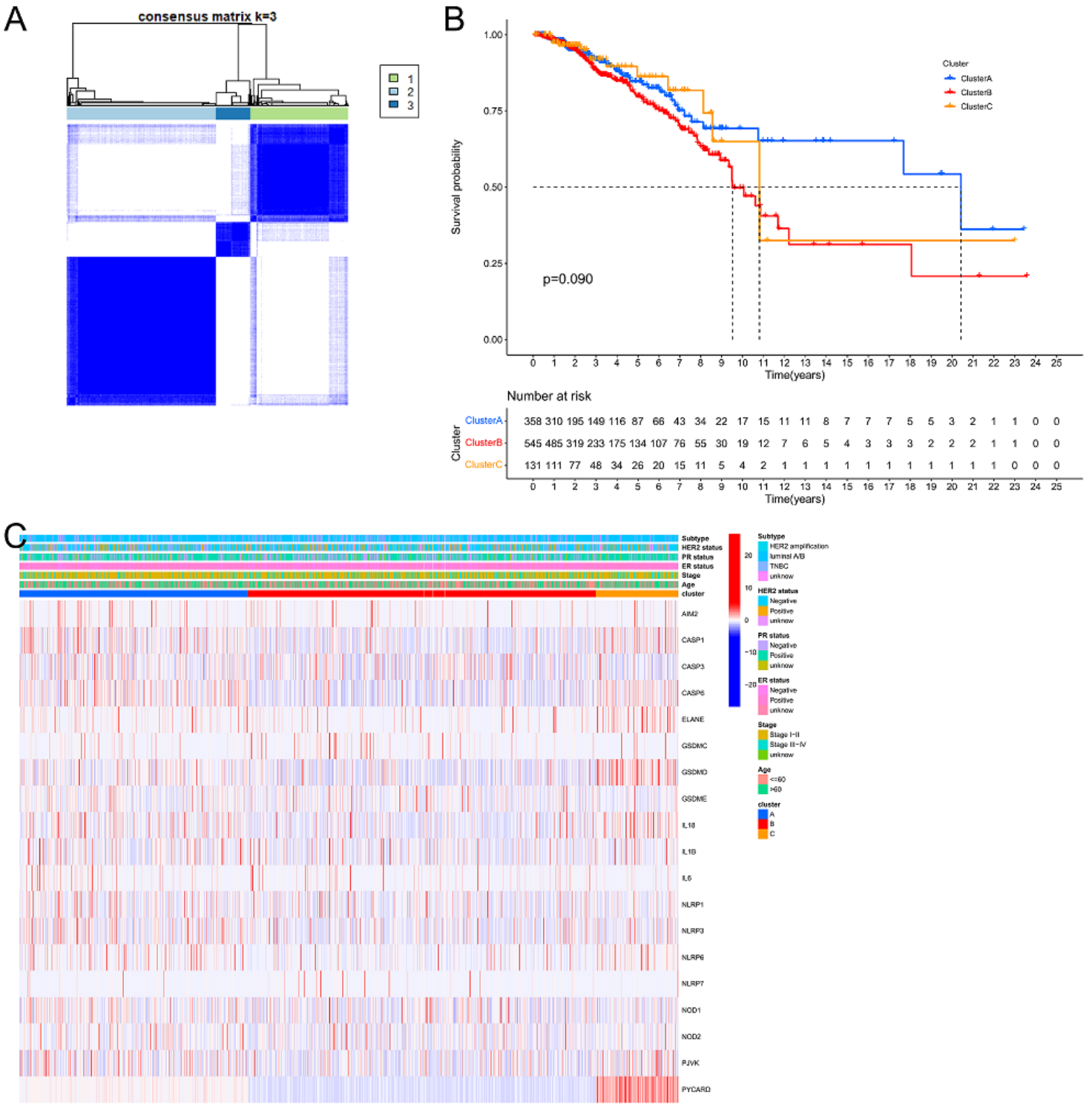

Figure 2

Tumour classification based on the pyroptosis-related DEGs. A 1085 BC patients were grouped into three clusters according to the consensus clustering matrix (k = 3). B Kaplan–Meier OS curves for the three clusters. C Heatmap and the clinicopathologic characters of the three clusters classified by these DEGs (Subtype:HER2 amplification, TNBC,luminal A/B).

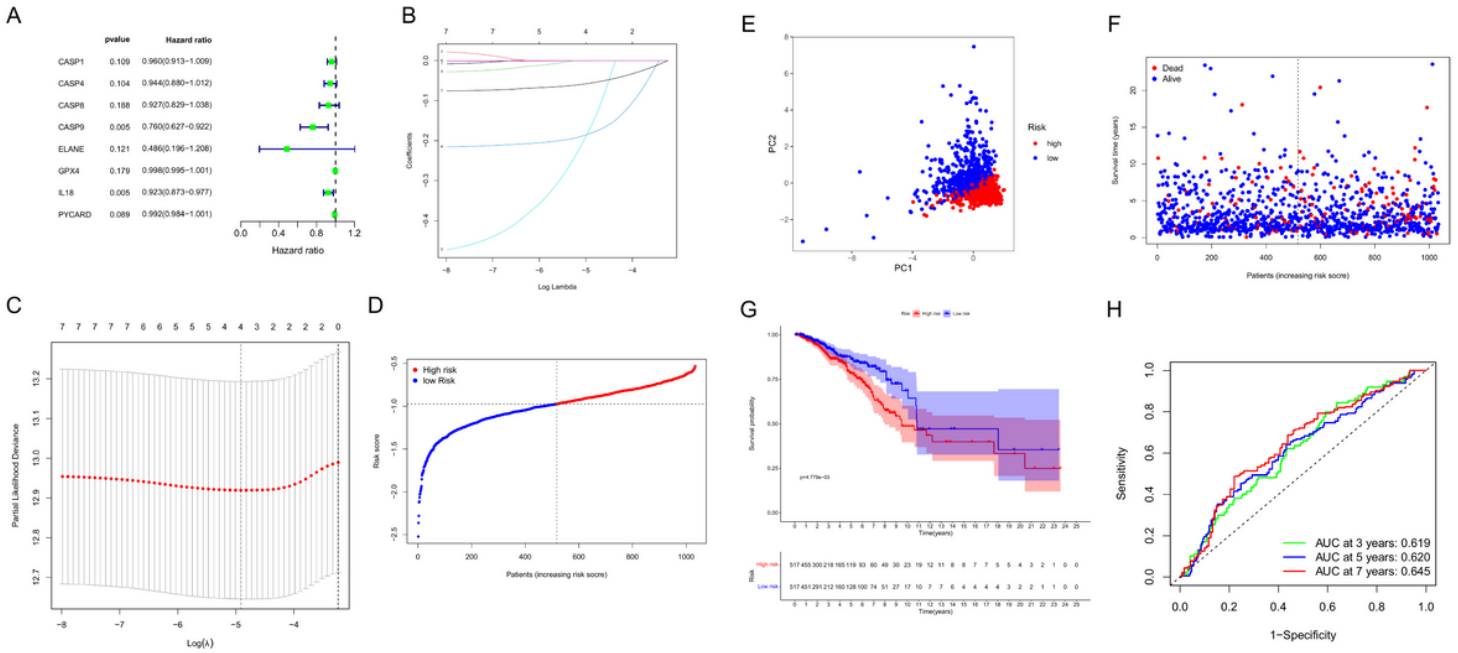

Figure 3

Construction of risk signature in the TCGA cohort. A Univariate cox regression analysis of OS for each pyroptosis-related gene, and 8 genes with P < 0.2. B LASSO regression of the 8 OS-related genes. C Cross-validation for tuning the parameter selection in the LASSO regression. D Distribution of patients based on the risk score. E PCA plot for BCs based on the risk score. F The survival status for each patient (low-risk population: on the left side of the dotted line; high-risk population: on the right side of the dotted line). G Kaplan–Meier curves for the OS of patients in the high- and low-risk groups. H ROC curves demonstrated the predictive efficiency of the risk score.

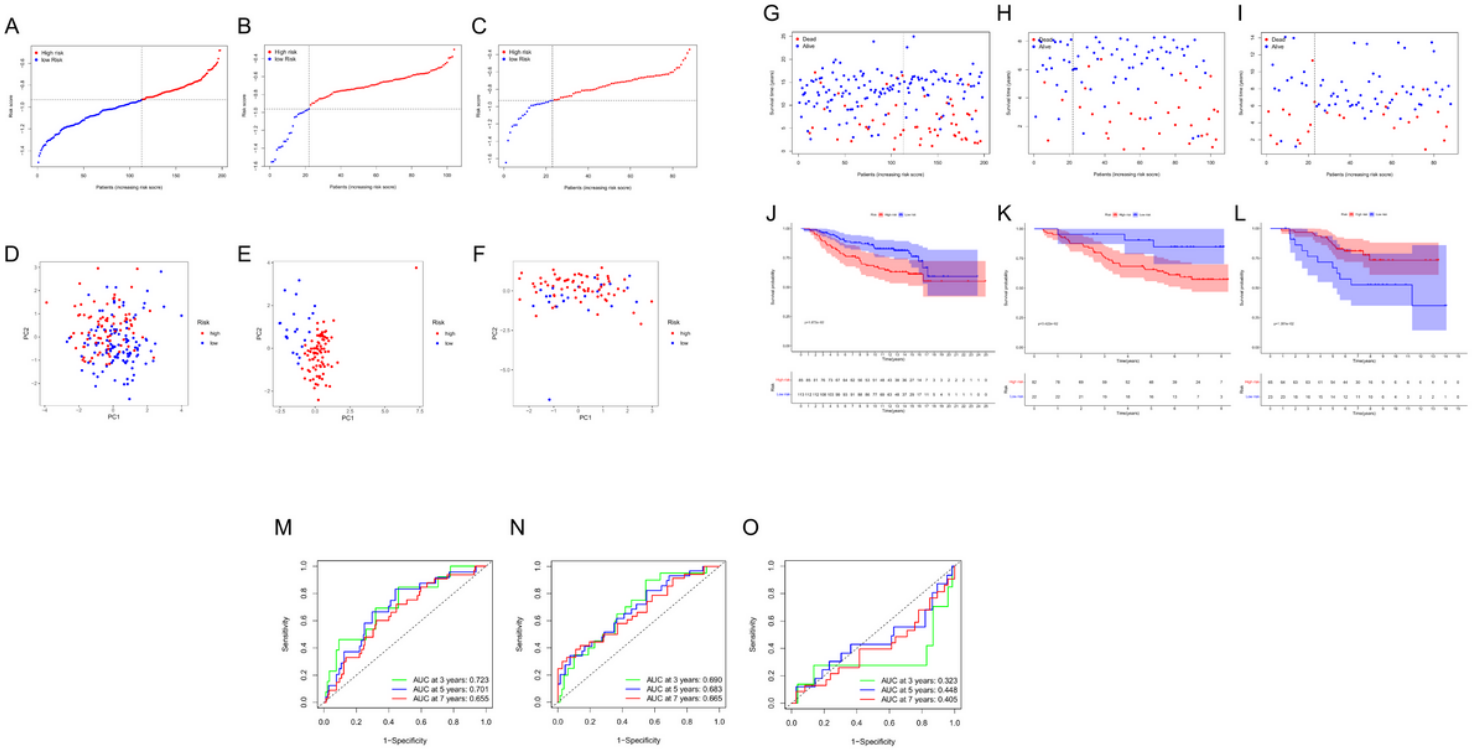

Figure 4

Validation of the risk model in the GEO cohort. A,B,C Distribution of patients in the GEO cohort(GSE7390, GSE42568,and GSE20713)based on the median risk score in the TCGA cohort. D,E,F PCA plot for BCs. G,H,I The survival status for each patient (low-risk population: on the left side of the dotted line; high-risk population: on the right side of the dotted line). J,K,L Kaplan–Meier curves for comparison of the OS between low- and high-risk groups. M,N,O Time-dependent ROC curves for BCs

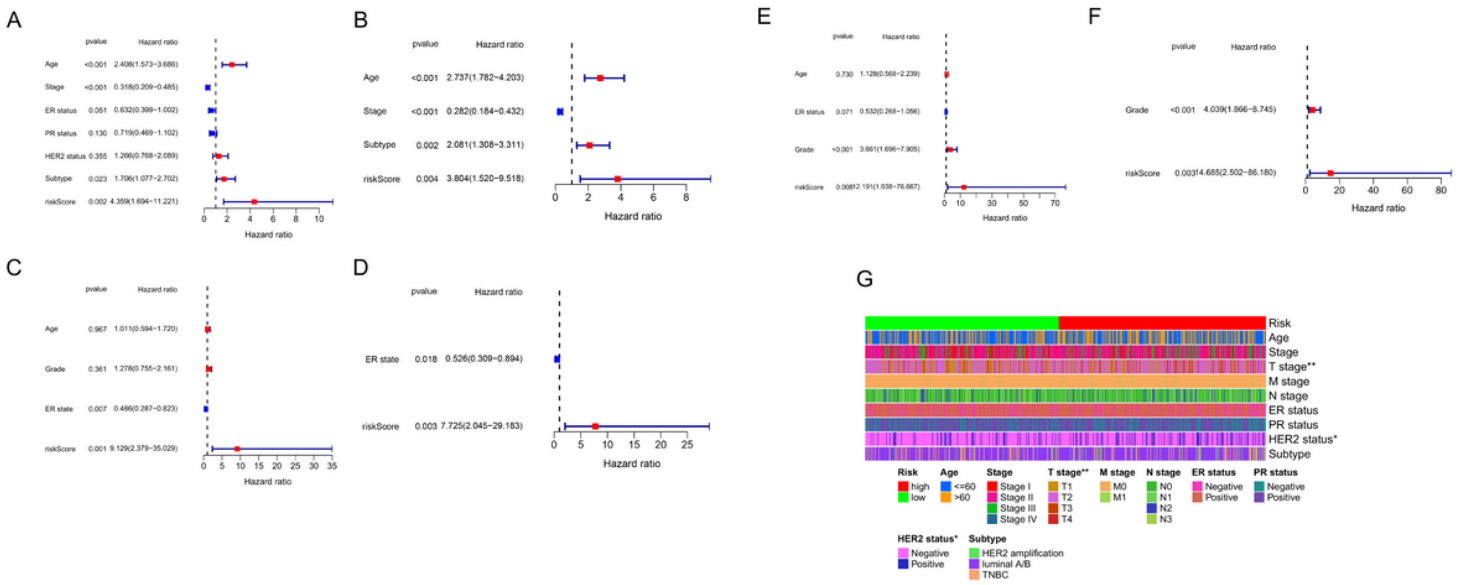

Figure 5

Univariate and multivariate Cox regression analyses for the risk score. A Univariate analysis for the TCGA cohort(Subtype:HER2 amplification, TNBC, luminal A/B). B Multivariate analysis for the TCGA cohort. C Univariate analysis for the GSE7390 cohort . D Multivariate analysis for the GSE7390 cohort. E Univariate analysis for the GSE42568 cohort . F Multivariate analysis for the GSE42568 cohort. G Heatmap (green: low expression; red: high expression) for the connections between clinicopathologic features and the risk groups (*P < 0.05,**P < 0.01).

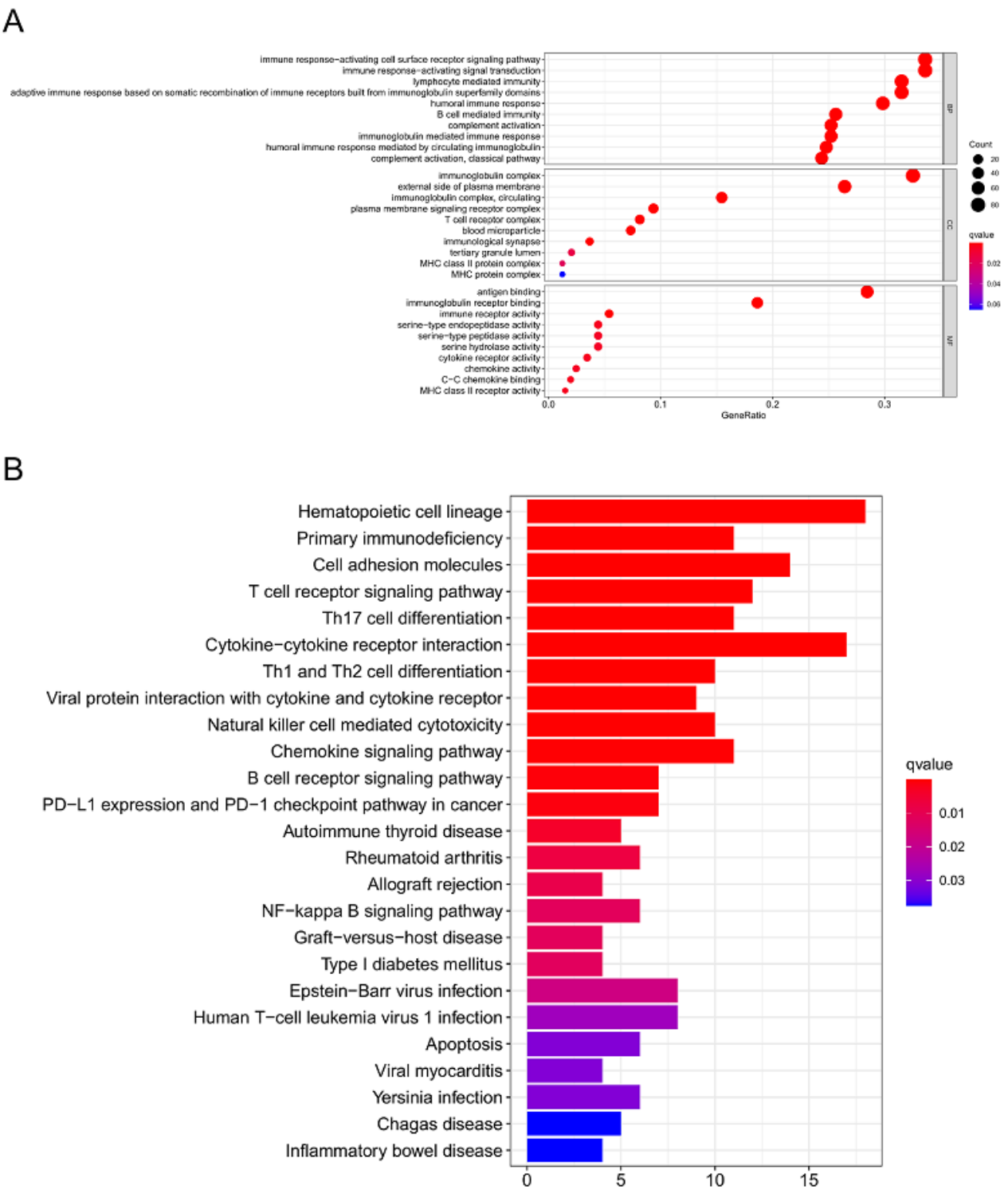

Figure 6

Functional analysis based on the DEGs between the two-risk groups in the TCGA cohort. A Bubble graph for GO enrichment (the bigger bubble means the more genes enriched, and the increasing depth of red means the differences were more obvious; q-value: the adjusted p-value). B Barplot graph for KEGG pathways (the longer bar means the more genes enriched, and the increasing depth of red means the differences were more obvious)

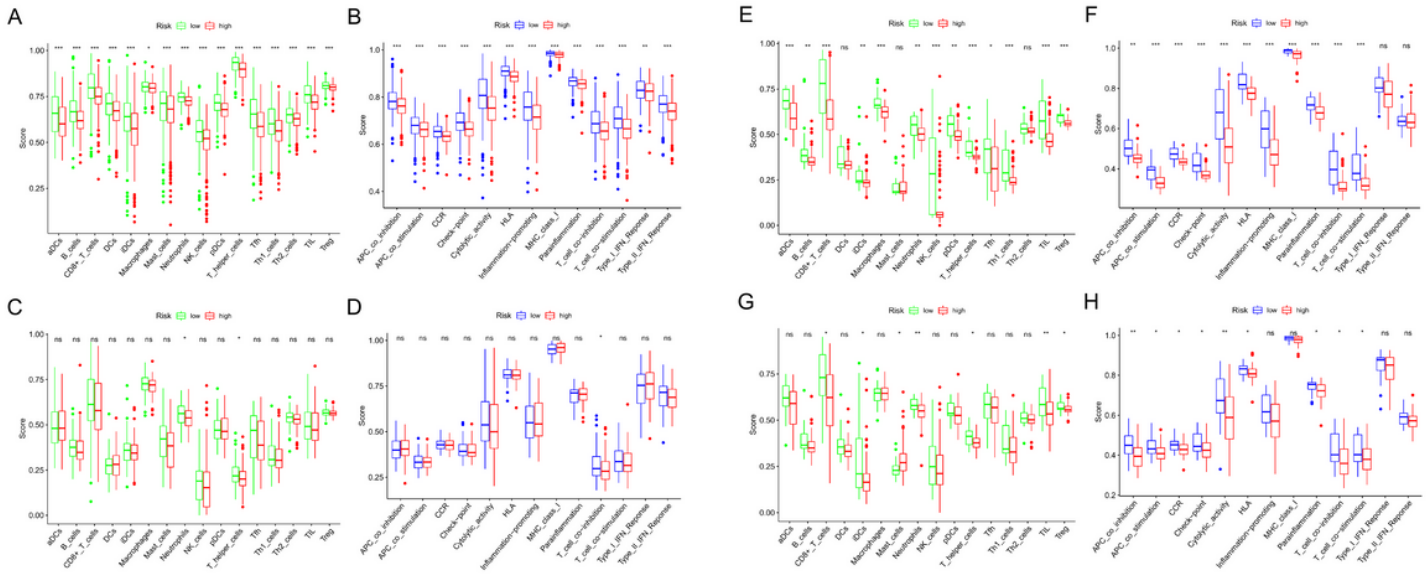

Figure 7

Comparison of the ssGSEA scores for immune cells and immune pathways. A, B Comparison of the enrichment scores of 16 types of immune cells and 13 immune-related pathways between low- and high-risk group in the TCGA cohort. C, D Comparison of the tumour immunity between low- and high-risk group in the GSE7390 cohort. E, F Comparison of the tumour immunity between low- and high-risk group in the GSE42568 cohort. G, H Comparison of the tumour immunity between low- and high-risk group in the GSE20713 cohort. P values were showed as: ns not significant; *P < 0.05;**P < 0.01; ***P < 0.001

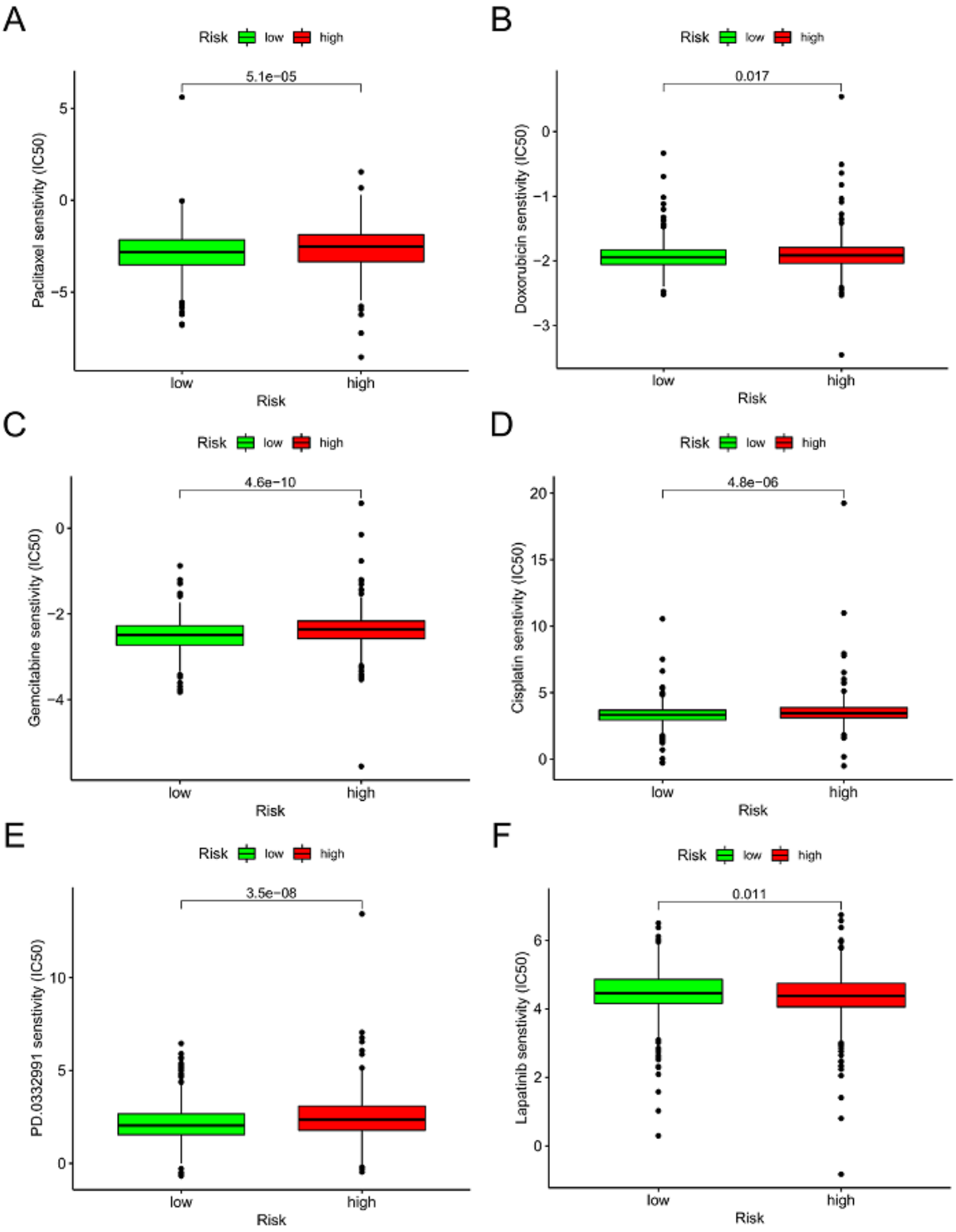

Figure 8

Correlation analysis between chemotherapeutic drugs and model. The model acted as a potential predictor for chemosensitivity.The low-risk group was associated with the lower IC50 of chemotherapy treatments, such as Paclitaxel, Doxorubicin, Gemcitabine, Cisplatin, and PD.0332991 (Palbociclib) , and the higher IC50 with Lapatinib.

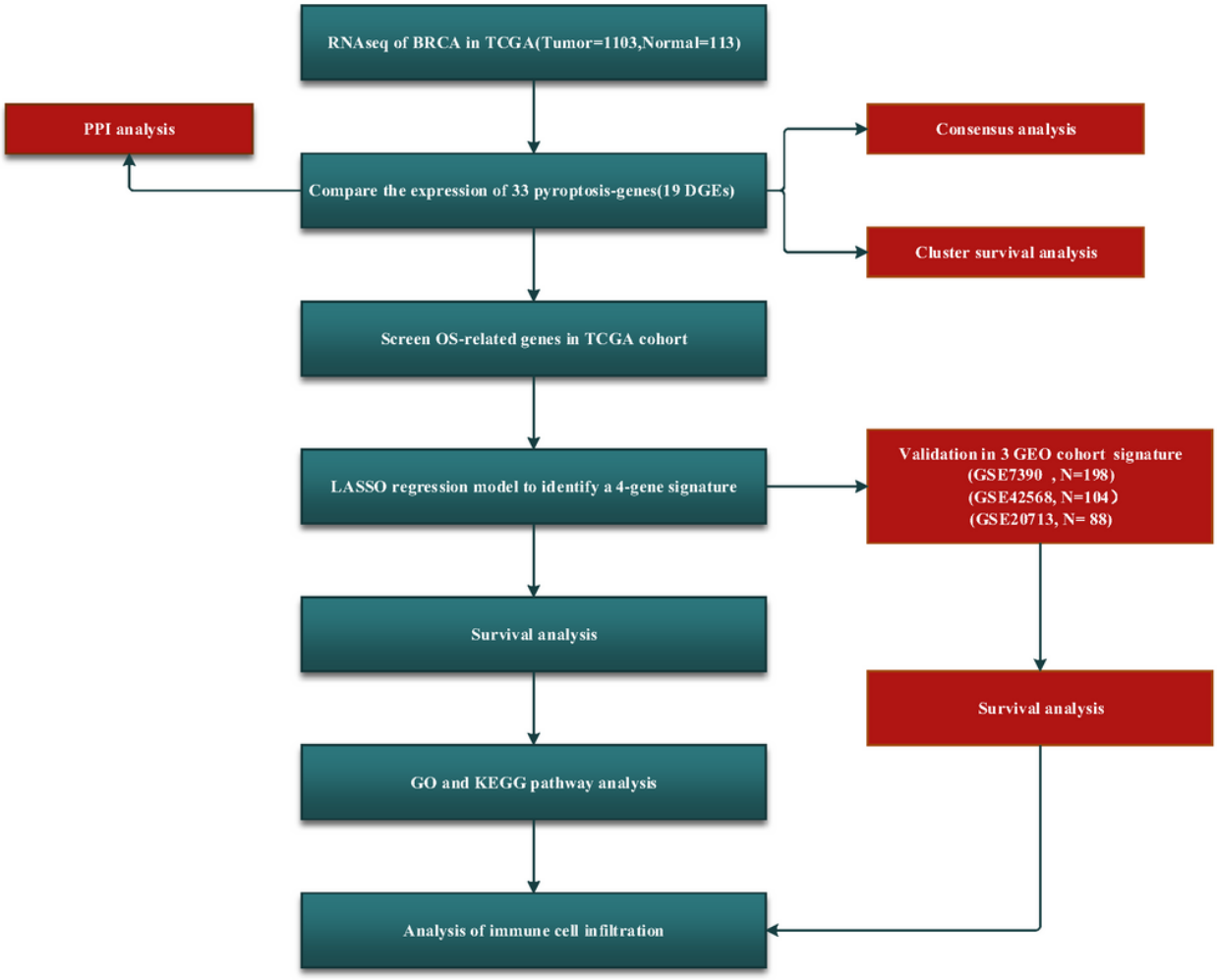

Figure 9

One-way analysis of variance was used to compare gene expression levels between normal patients and breast cancer patients, and the Pearson chi-square test was selected as the categorical variable.

Supplementary Files

This is a list of supplementary files associated with this preprint. Click to download.

- TableS1.xlsx
- TableS3.txt